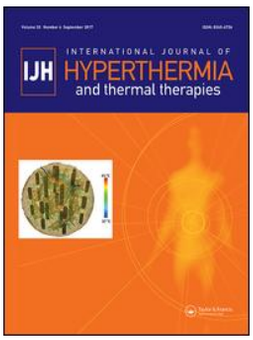

International Journal of Hyperthermia

ISSN: 0265-6736 (Print) 1464-5157 (Online) Journal homepage: https://www.tandfonline.com/loi/ihyt20

Standardization of patient modeling in hyperthermia simulation studies: introducing the *Erasmus Virtual Patient Repository*

Gennaro G. Bellizzi, Kemal Sumser, Iva VilasBoas-Ribeiro, Sergio Curto, Tomas Drizdal, Gerard C. van Rhoon, Martine Franckena & Margarethus M. Paulides

To cite this article: Gennaro G. Bellizzi, Kemal Sumser, Iva VilasBoas-Ribeiro, Sergio Curto, Tomas Drizdal, Gerard C. van Rhoon, Martine Franckena & Margarethus M. Paulides (2020) Standardization of patient modeling in hyperthermia simulation studies: introducing the *Erasmus Virtual Patient Repository*, International Journal of Hyperthermia, 37:1, 608-616, DOI: 10.1080/02656736.2020.1772996

To link to this article: https://doi.org/10.1080/02656736.2020.1772996

Published online: 09 Jun 2020.

INTERNATIONAL JOURNAL OF HYPERTHERMIA
2020, VOL. 37, NO. 1, 608–616
https://doi.org/10.1080/02656736.2020.1772996

Taylor & Francis
Taylor & Francis Group

Standardization of patient modeling in hyperthermia simulation studies: introducing the *Erasmus Virtual Patient Repository*

Gennaro G. Bellizzi[a], Kemal Sumser[a], Iva VilasBoas-Ribeiro[a], Sergio Curto[a], Tomas Drizdal[b], Gerard C. van Rhoon[a], Martine Franckena[a] and Margarethus M. Paulides[a,c]

[a]Hyperthermia Unit, Department of Radiation Oncology, Erasmus University Medical Center, Rotterdam, The Netherlands; [b]Department of Biomedical Technology, Czech Technical University in Prague, Prague, Czech Republic; [c]Department of Electrical Engineering, Eindhoven University of Technology, Eindhoven, The Netherlands

ABSTRACT

Purpose: Thermal dose-effect relations have demonstrated that clinical effectiveness of hyperthermia would benefit from more controlled heating of the tumor. Hyperthermia treatment planning (HTP) is a potent tool to study strategies enabling target conformal heating, but its accuracy is affected by patient modeling approximations. Homogeneous phantoms models are being used that do not match the body shape of patients in treatment position and often have unrealistic target volumes. As a consequence, simulation accuracy is affected, and performance comparisons are difficult. The aim of this study is to provide the first step toward standardization of HTP simulation studies in terms of patient modeling by introducing the *Erasmus Virtual Patient Repository* (EVPR): a virtual patient model database.
Methods: Four patients with a tumor in the head and neck or the pelvis region were selected, and corresponding models were created using a clinical segmentation procedure. Using the Erasmus University Medical Center standard procedure, HTP was applied to these models and compared to HTP for commonly used surrogate models.
Results: Although this study was aimed at presenting the EVPR database, our study illustrates that there is a non-negligible difference in the predicted SAR patterns between patient models and homogeneous phantom-based surrogate models. We further demonstrate the difference between actual and simplified target volumes being used today.
Conclusion: Our study describes the EVPR for the research community as a first step toward standardization of hyperthermia simulation studies.

ARTICLE HISTORY
Received 12 December 2019
Revised 19 May 2020
Accepted 19 May 2020

KEYWORDS
Hyperthermia; patient models; treatment planning; open research; standardization

1. Introduction

Clinical and biological studies have shown the benefit of hyperthermia as an additive to radiotherapy and chemotherapy [1–5]. Given the demonstrated thermal dose-effect relations, clinical effectiveness would greatly benefit from achieving more controlled temperatures; especially in mild hyperthermia where homogeneous and target conformal heating in the range between 42 and 43 °C is considered optimal [6–10]. Temperature monitoring is currently performed using invasive catheters and thus limited to a few measurement points or not applied at all due to patient discomfort. This makes it difficult to verify the three-dimensional (3D) temperature distribution during treatment. A promising approach to overcome these clinical challenges is hyperthermia treatment planning (HTP), which offers potential for pretreatment and real-time optimization of heating settings, parametric studies and the design of new applicators [11].

In HTP simulation studies, it is common practice to use computer-aided design (CAD) models of healthy volunteers and homogeneous phantoms with anatomical shapes [12–19]. These models, while readily available, often are not representative of the hyperthermia patient models in terms of anatomy, posture and target shape. Hence, the results of many studies may be biased due to the use of these surrogate models, but the true impact of this bias is unknown. In addition to that, comparisons amongst different studies are difficult and of questionable relevance because of the different models being used.

HTP has been used to study several novel technologies, such as antenna concepts [20–22], applicator designs [23–25] and optimization approaches for real-time optimization of treatment settings [26–29]. Such simulation studies are often conducted using segmented anatomies of healthy humans or simplified homogeneous anatomies [12,13,17–19,30,31]. Since the early '70s, researchers worked on developing 3D human models with diverse levels of detail. The advent of computerized tomography (CT) and magnetic resonance

CONTACT Gerard C. van Rhoon g.c.vanrhoon@erasmusmc.nl Hyperthermia Unit, Department of Radiation Oncology, Erasmus University Medical Center, Rotterdam, The Netherlands

imaging (MRI) resulted in the development of several high-resolution 3D segmented anatomies derived from data of healthy volunteers [32–38]. Besides some value of these models, they are based on healthy volunteers or simplified homogeneous anatomies and lack specific features of hyperthermia patient models, such as body shape conforming to the treatment positioning and clinician-delineated tumor volume. Despite the partially known impact of these approximations, a standard set of patient models intended for HTP purposes is not available.

Numerous HTP simulation studies were unable to properly capture relevant features of patient models in simplified surrogate models. In [39], a layered phantom model was shown to be unrepresentative of patient anatomies for clinical comparison purposes since the fat-muscle transitions were unrealistic. Similarly, de Bruijne et al. [40] and Trujillo-Romero et al. [41] have shown the non-negligible impact on the specific absorption rate (SAR) of using simplified anatomies as opposed to patient models (including metallic parts). Moreover, although there is no consensus on the optimal tissue list for segmentation, Kok and coworkers [42] mentioned that high dielectric contrast interfaces (bone, fat, muscle tissue) have a significant influence on the predicted temperature distribution. All of these studies demonstrate that homogeneous phantoms cannot be considered appropriate surrogates for patient models. In addition, the presence of an invading tumor may further affect simulation results.

Other items affecting simulation accuracy are the treatment posture and the presence of a tumor volume. The 3D segmented anatomies derived from healthy volunteers [32–38] do not include an invading tumor. The non-negligible impact of this has been demonstrated in a head and neck tumor patient, where the predicted SAR distribution in the tumor was overestimated due to the lack of a region with tumor properties in the patient model [43]. In the case of deep pelvic hyperthermia, it was shown that HTP results are strongly affected by the combination of the tumor position and the shape of the patient body [44,45]. Finally, Paulides et al. [11] extracted the need for modeling setups matching the clinical scenario, when aiming for hotspot prevention in the development of novel HT applicators. Hence posture and the presence of the tumor are also important to take into account.

The aim of this study is to stimulate open research by creating a common ground for hyperthermia simulation studies in terms of patient modeling. Models of representative patients with different target locations and sizes and that have been treated with hyperthermia were selected. Two models were created based on patients suffering from a tumor in the head and neck (named Alex, Murphy) and two were created since they had a tumor in the pelvic region (named Clarice, Will). These CAD models are stored in a novel, openly accessible database called the *Erasmus Virtual Patient Repository* (EVPR). For the selected models, we illustrate the impact of realistic patient modeling by comparing the predicted SAR distributions for approximated models to results for the EVPR database. To illustrate the impact of realistic target shape, we imported clinician-delineated targets into corresponding locations in the two homogeneous phantom CAD models. We then proceeded to compare HTP results with those of approximated (spherical or elliptical) targets of the same volume. SAR-based HTP was performed for all models in accordance with the clinical procedure at Erasmus MC Cancer Institute [29].

2. Materials and methods

2.1. Patient models

Four patient CAD models were created using the clinical segmentation procedure as follows. For head and neck patient models, HTP is based on CT scans made for radiotherapy treatment planning. However, deep pelvic HTP is based on CT scans made in a tailored sling (PYREXAR Medical, Salt Lake City, UT). As such, the patient models are generated in the exact same position and with the same body shape as during the hyperthermia treatment [46–48]. The 3D models were created by delineating scans into normal tissues and the target volume using a semi-automatic segmentation routine followed by a manual adjustment in software tool iSeg (Zurich Medtech, Zurich, Switzerland) [46]. For each case, a trained clinician identified the hyperthermia target volume (HTV) starting from the clinical target volume (CTV) for radiotherapy treatment and adding certain margins depending on the specific case [49,50]. These models constitute the EVPR database and are depicted in Figure 1 and details are reported in Table 1.

The male head and neck patient model named Murphy is based on a patient with an oropharynx tumor (∼35 ml), and the model named Alex is based on a patient with a more challenging case of a deeper-seated nasopharynx tumor (∼44 ml). The Murphy model was treated after surgery and therefore only includes the HTV and no CTV (no solid tumor mass). The deep pelvic patient model named Clarice is based on a female patient with a cervix tumor (∼120 ml), and the deep pelvic model named Will is based on a male patient with a more challenging rectum tumor having irregular contours and a large volume (∼430 ml). Note that for both Clarice and Will the HTV coincides with the CTV from radiotherapy planning. Density and electromagnetic properties at different applicator operating frequencies are reported in Table 2.

2.1.1. Representativeness of adopted 3D patient models

The EVPR database models were chosen to represent the patient population regularly treated, taking into account the experience of our group in HTP. We are aware that this dataset should be the beginning of an actual patient model's repository that covers all of the most important variations in patient and HTV characteristics. For the head and neck models, we considered both a model including a solid tumor mass, Alex model, and a model which does not include it, Murphy model. The Murphy model case is a less common but realistic case. Its target constitutes multiple tissues that are at high risk after the gross tumor was removed by surgery. Furthermore, Alex includes one of the most challenging

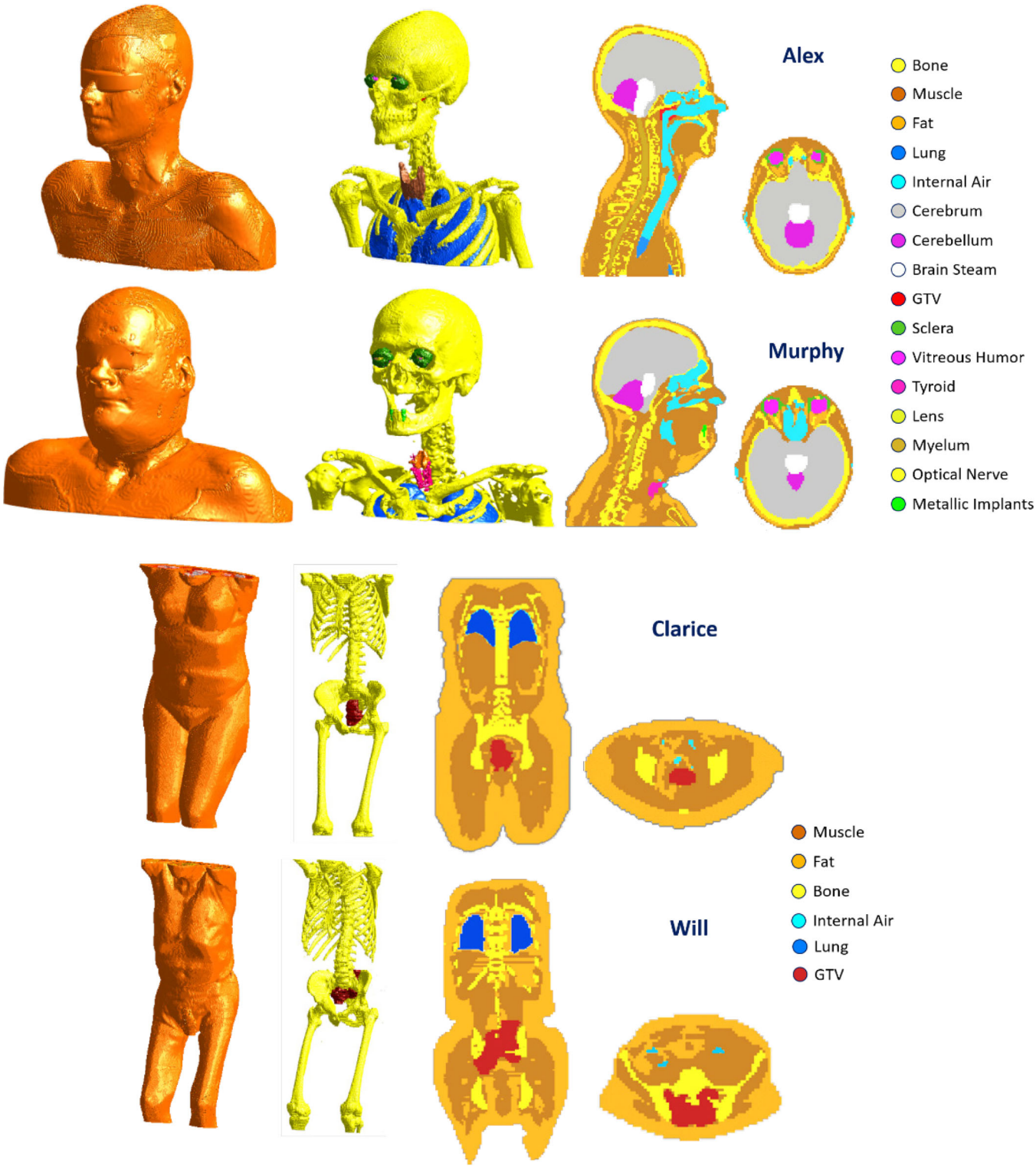

Figure 1. The *Erasmus Virtual Patient Repository*: Alex, Murphy, Clarice and Will CAD models.

Table 1. Anatomical details of the patient models included in the EVPR database.

Model/info	Tumor location	HTV volume
Murphy	Oropharynx	35 ml
Alex	Nasopharynx	44 ml
Clarice	Cervix	120 ml
Will	Rectum	430 ml

target volumes: a deep-seated nasopharynx tumor, shown in Figure 2. On the other hand, stands the Murphy model, which includes a target volume and location that is easier to heat, but is challenging due to the presence of metallic teeth implants that can cause local SAR hotspots. Similar reasoning drove the selection of the deep pelvic models. Clarice and

Table 2. List of the electromagnetic properties at 434 MHz and 77 MHz and density of all tissues included in Will, Clarice, Alex and Murphy CAD models [29].

Name	Frequency (MHz)	Relative permittivity	Electrical conductivity (S/m)	Density (kg/m^3)
Bone	434	13.07	0.09	1908
	77	16.00	0.06	
Fat	434	11.59	0.08	911
	77	13.20	0.07	
Muscle	434	56.86	0.80	1090
	77	69.30	0.69	
Lung	434	23.58	0.38	394
Cerebrum		56.81	0.75	1045
Brain stem		55.11	1.04	1046
Myelum		35.03	0.45	1075
Sclera		57.37	1.01	1032
Lens		37.28	0.37	1076
Vitreous humor		68.99	1.53	1005
Cartilage		45.14	0.59	1100
Thyroid		61.32	0.88	1050
Optical nerve		35.03	0.45	1075
GTV	434	59.00	0.89	1050
	77	69.00	0.70	

Figure 2. Sagittal and transversal view of the *Erasmus Virtual Patient Repository* CAD models enlightening the gross tumor volume (GTV) and/or the hyperthermia target volume (HTV) location within bone structures. In the case of Murphy, the HTV, in pink, is reported as no solid GTV is present.

Will exhibit different fat percentages and body sizes, i.e., almost a twofold difference. As shown in Figure 2, Clarice is representative of a target with a regular shape and volume which is easier to heat, while Will includes a larger and irregular target volume that surrounds the pubic bones.

2.1.2. 3D model volume anonymization for privacy compliance

In order to comply with current privacy regulation and be able to share the described patient models, no information possibly identifying the single models of the EVPR database can be shared [51]. To this end, anonymization of the 3D voxel model was needed for both Alex and Murphy. A non-isotropic volume expansion of the muscle tissue has been added with the aim of covering the eyes. This added layer, shown in Figure 1, hides the eye structures and shapes to avoid any possible link to the individual. We verified that this added layer did not affect the HTP metrics.

2.2. HTP workflow

The first step for HTP includes segmenting the 3D patient models. The patient-specific models were imported into Sim4Life (Zurich MedTech AG, Zurich, Switzerland) along with the related 3D applicator model. The HYPERcollar3D, operating at 434 MHz, was used for the head and neck patients [43] and the Pyrexar BSD2000 Sigma 60 applicator (Pyrexar Medical Corp., Salt Lake City, UT), operating at 77 MHz, [52,53] was used for the patients with a deep pelvic tumor. Electromagnetic tissues properties for these frequencies were assigned to each of the segmented tissues and are presented in Table 2. The water bolus was modeled by a water volume with relative permittivity of 80 and conductivity of 0.04 S/m for 434 MHz and 0.003 S/m for 77 MHz between the patient and the applicator shell. The total field was computed for a 1 V sinusoidal signal excitation and 20 periods of harmonic signal for each antenna at the operating frequency. The electric field per antenna was normalized to 1 W radiated power and the cubic filtered SAR (cf-SAR) pattern optimized using our *Visualization Tool for Electromagnetic Dosimetry and Optimization* (VEDO) software [29]. The optimization strategy implemented in VEDO aims at maximizing the Target to Hotspot Quotient (THQ), which is expressed as:

$$THQ = \frac{<SAR>_{HTV}}{<SAR>_{hot-spot}}$$

where $<SAR>_{HTV}$ is the average SAR within the target volume and $<SAR>_{hot-spot}$ is the average SAR at the hot-spot, which is defined as the cumulative 1% volume in all healthy tissues with the highest SAR. Particle swarm optimization scheme was used to maximize the THQ cost function. The HTV was used as optimization target volume. A more detailed description of HTP can be found in [29,50].

2.3. Comparison with realistic representative models

The EVPR database models were compared to realistic representative modeling approaches, which are described below

and are inspired by the strategies commonly used in literature to mimic patient models. In the following investigation, we considered simplified homogeneous anatomies including ellipsoidal target volumes or clinician-delineated HTV. The HTP quality parameters achieved for these surrogate models were compared to those of the EVPR database.

The effect of the tissue distribution has been investigated using homogenous models. We included two in-house developed patient modeling phantoms for deep pelvic and head and neck tumors. Homogeneous electromagnetic properties were assumed except for the HTV. The HENK phantom consists of a human-shaped shell containing bone structure resembling a human spine and pelvis embedded into homogenous dielectric material with permittivity equal to 69.3 and conductivity 0.69 S/m at 77 MHz [54]. The ADAM phantom, 'Anthropomorphic Dosimetry head And neck Mannequin', was obtained as the average shape of 30 head and neck patient models and it does not have any bone structures. We used a relative permittivity of 41 and a conductivity of 0.50 S/m at 434 MHz.

The impact of using an actual clinician-delineated HTV was investigated by including both the actual HTV and an ellipsoidal target volume within both ADAM and HENK. These generic target volumes had the same volume of the clinician-delineated HTV and have been places at the same position of the clinician-delineated HTV. Note that the HTP workflow was performed for each approximated model (ADAN and HENK) and each target shape (HTV and approximated elliptical target) and compared to the EVPR database models.

2.4. Evaluation metrics

In order to quantify the differences between the two patient model approaches, we used two standard HTP SAR quality metrics: THQ and target coverage. The THQ has been defined in Section 2.2. The target coverage is defined as the percentage of the target volume which is above a certain percentage of the maximum SAR induced within the patient model. We considered target coverage above 25% and 50% of the maximum and we indicated these as TC25 and TC50, respectively.

These metrics are currently used for clinical decision making for head and neck, superficial and deep pelvic patients. Canters et al. [55] used the predicted temperature parameters as a basis for selecting a set of quality indicators and optimization functions for deep pelvic hyperthermia, applied with the BSD2000 Sigma 60 applicator also used here. Their results showed the THQ as being most predictive for median target temperature, T50. Earlier, a relation was found between the target coverage of the TC25 and clinical outcome for superficial hyperthermia [56]. Recently, for the case of head and neck cancer treated with HYPERcollar3D, Bellizzi et al. [57] identified TC50 as best temperature surrogate related to median target temperature. Assessing differences in terms of these quantities will reflect on predicted temperature and hence on treatment outcome [58,59].

3. Results

3.1. Impact of the anonymization volume for Alex and Murphy

The maximum difference in terms of SAR quality metrics was found in target coverage and it deviates 1% for the not anonymized vs. the anonymized volumes. Note that only ~0.17% of the whole model volume was added. Figure 3 depicts two sagittal views of the normalized SAR distribution induced in both not anonymized and anonymized Murphy where the maximum qualitative difference was observed.

3.2. Impact of target modeling

Tables 3–6 report the SAR quality metrics obtained for the EVPR database models compared to the homogeneous phantom models including both simplistic and target volumes delineated by clinicians. The SAR quality metrics achieved with the EVPR database were compared to two different

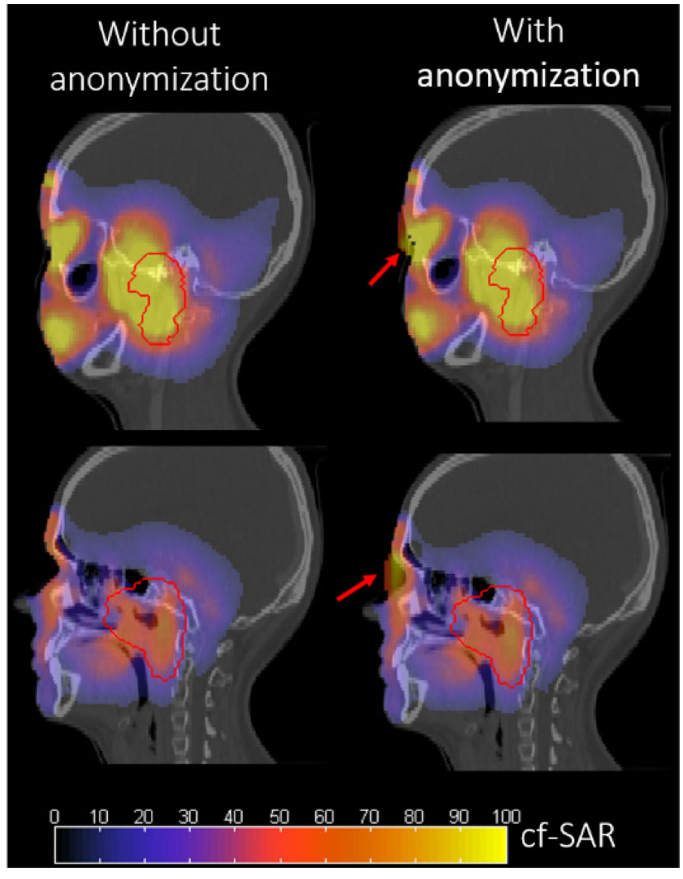

Figure 3. Sagittal views of the normalized SAR distributions achieved when performing HTP in Murphy's before and after CAD model anonymization through eyes structure morphing. The red arrows indicate the location of the maximum difference in the SAR.

Table 3. SAR-based quality metrics for the Alex model (head and neck) including a nasopharynx HTV compared to ADAM including the Alex's nasopharynx HTV and a volume- and position-matched spherical target volume.

Model	TC25 (%)	TC50 (%)	THQ (–)
ADAM + generic target	100	100	1.14
ADAM + HTV	100	100	1.34
Alex	94	71	1.21

Table 4. SAR-based quality metrics for the Murphy model (head and neck) including an oropharynx HTV compared to ADAM including the Murphy's oropharynx HTV and a volume- and position-matched spherical target volume.

Model	TC25 (%)	TC50 (%)	THQ (–)
ADAM + generic target	97	64	0.68
ADAM + HTV	58	24	0.38
Murphy	46	16	0.36

Table 5. SAR-based quality metrics for the Clarice model (pelvis) including a cervix HTV compared to HENK including Clarice's cervix HTV and a volume- and position-matched spherical target volume.

Model	TC25 (%)	TC50 (%)	THQ (–)
HENK + generic target	100	99	0.70
HENK + HTV	100	97	0.70
Clarice	81	0	0.48

Table 6. SAR-based quality metrics for the Will model (pelvis) including a cervix HTV compared to HENK including Will's cervix HTV and a volume- and position-matched spherical target volume.

Model	TC25 (%)	TC50 (%)	THQ (–)
HENK + generic target	100	91	0.70
HENK + HTV	99	84	0.70
Will	85	39	0.71

modeling approaches with increasing complexity. While Tables 3–6 report the SAR quality metric values, in the following we aimed at briefly report on the effect of using simplistic modeling as opposed to patient modeling. Specifically, comparing the EVPR database planning metrics with those for the homogeneous phantoms (ADAM and HENK), we found:

1. In case of a spherical/elliptical target, an average difference of $|\Delta TC25| = 21\%$, $|\Delta TC50| = 57\%$ and $|\Delta THQ| = 0.16$.
2. In the case of realistic target (HTV), an average difference $|\Delta TC25| = 28\%$, $|\Delta TC50| = 13\%$ and $|\Delta THQ| = 0.09$.

where $|\Delta X|$ is equal to $|X_1 - X_2|$ and X_1 and X_2 represent the SAR quality metrics for the different cases.

For qualitative observations besides the SAR quality metrics, Figure 4 depicts both a transversal and a sagittal cross-section of the normalized cf-SAR distributions induced in Clarice and Alex as compared to the above-mentioned surrogate models. When comparing the power deposition pattern achieved within ADAM and HENK as compared to the EVPR database models, the focus location appears at the HTV location, whereas the homogeneous tissue-mimicking-material yields to a smooth and unrealistic distribution. Finally, the tissue segmentation yields to different SAR distribution and hence to different hot-spot locations (potentially, to organs at risk or more sensitive areas) when comparing Ella or Duke with the EVPR database models.

4. Discussion

This work shows the impact of modeling based on patient anatomy segmentation and including clinician-delineated HTVs for simulation guided research purposes. Our analysis aimed at showing the differences of using surrogate models with arbitrary shaped target volumes instead of patient

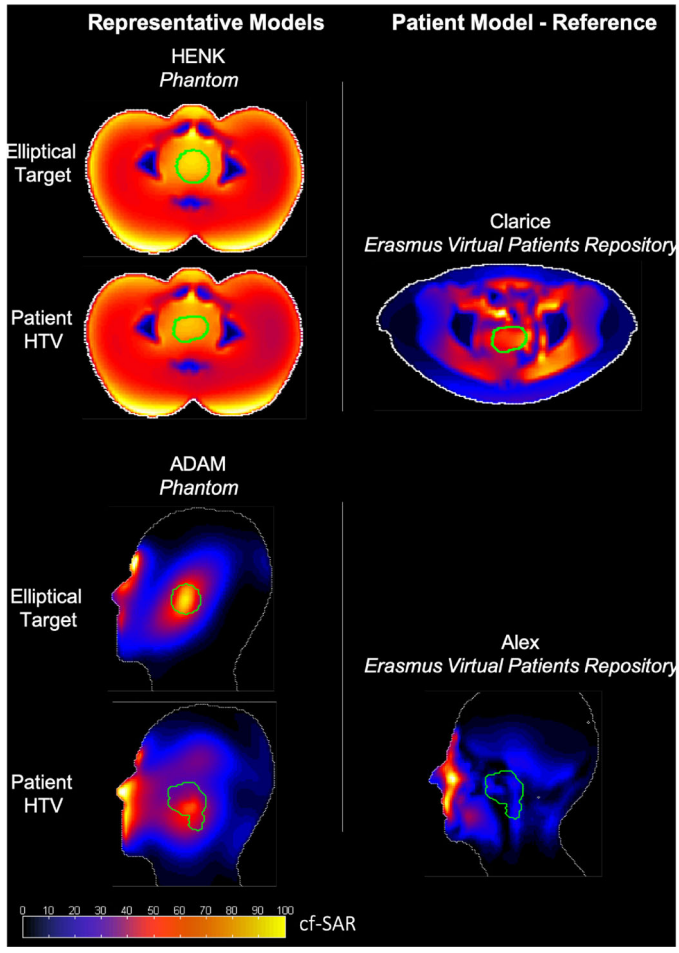

Figure 4. Transversal view through the HTV mid-line (green contour) of the SAR distributions predicted for the different patient model approximations and Clarice and Alex from the *Erasmus Virtual Patients Repository*, respectively.

models. In our analyses, we used SAR quality parameters that are used at Erasmus MC for clinical decision making during hyperthermia treatments as they correlate to predicted temperature for both deep [55] and head and neck hyperthermia [57].

From a qualitative point of view, Figure 4 suggests the use of homogenous phantom modeling as first step in simulation studies because of the good predictability and measurability of SAR patterns into phantoms for quality assurance purposes. However, these homogeneous phantom models are not representative of patient models, as excessively smooth and not realistic SAR patterns are observed. Therefore, virtual studies should be based on patient-specific modeling, as surrogate models inevitably lead to modeling inaccuracies. Clinician-delineated target volumes and models of patients in treatment position need to be used for in simulation studies [44,45]. Hence, while simplistic modeling might be useful first step in simulation-guided technology development, final tests and conclusion should be drawn on actual clinical models.

Although we focused our attention on SAR quality metrics in our investigations, the findings are consistent in terms of predicted temperature too, as was shown previously [55,57]. For the case of head and neck cancer treated with HYPERcollar3D, Bellizzi et al. [57] demonstrated in a

simulation study that the TC50 is the optimal temperature surrogate, which is correlated to median predicted target temperature (T50). For the case of deep pelvic cancer treated with the BSD2000 Sigma 60 applicator, Canters et al. [55] distinguished the THQ as most predictive for predicted T50. According to these studies, the differences in the predicted SAR quality indicators found in the proposed initial study, would translate into a variation in median predicted HTV temperature T50 greater than 0.75 °C [58,59]. However, open discussions are still ongoing regarding the impact of this on clinical effectiveness. In this work, we have chosen not to include temperature simulation, as SAR is usually the first step of technology development as it is the more straightforward indicator of the field propagation and blood perfusion mechanisms are not fully known. The open debate regarding thermal properties as well as the unknown clinical outcome of such improvements in predicted median temperature could lead to different interpretations of the results.

The results of our work motivated us in sharing the EVPR database with the hyperthermia community. Our work has been mainly focused on the HTP. However, the provided models can also be used for research into applications in which a segmented patient anatomy is needed, like electrical properties tomography (EPT) and focused ultrasound (FUS).

5. Conclusion

The aim of this study was to present and analyze the EVPR database. This database includes four models of patients undergoing hyperthermia for a tumor in the head and neck (two) or pelvic region (two). The impact of anonymization measures was found to be less than 1%-point for all HTP metrics, i.e., TC25, TC50 and THQ. The impact of both a realistic posture and fat-muscle-bone discontinuities has been shown by comparing homogenous phantom modeling with patient models. The impact of using an actual delineated target (HTV) vs. an approximated target (sphere/ellipse) was 1–51% in TC25, 8–52% in TC50 and 0.01–0.32 in THQ.

The EVPR database forms a realistic database of models from patients in treatment position for hyperthermia simulation studies. These models allow to accelerate technology developments by enabling faster and better comparisons based on a common benchmark. Details for data transfer agreement and downloads can be arranged via the corresponding authors as well as through the European Society of Hyperthermic Oncology (ESHO) webpage.

Disclosure statement

No potential conflict of interest was reported by the author(s).

Funding

This work was performed within the framework of COST Action MYWAVE, supported by COST (European Cooperation in Science and Technology) and financially supported by the Dutch Cancer Society (project 11368) as well as the Netherlands Organisation for Scientific Research (NWO) (project STW15195).

ORCID

Gennaro G. Bellizzi http://orcid.org/0000-0003-2866-2973
Kemal Sumser http://orcid.org/0000-0002-6695-2659
Tomas Drizdal http://orcid.org/0000-0001-9061-8231

References

[1] Datta NR, Ordóñez SG, Gaipl US, et al. Local hyperthermia combined with radiotherapy and-/or chemotherapy: recent advances and promises for the future. Cancer Treat Rev. 2015;41(9):742–753.
[2] Datta NR, Rogers S, Ordóñez SG, et al. Hyperthermia and radiotherapy in the management of head and neck cancers: a systematic review and meta-analysis. Int J Hyperthermia. 2016;32(1):31–40.
[3] Kampinga HH. Cell biological effects of hyperthermia alone or combined with radiation or drugs: a short introduction to newcomers in the field. Int J Hyperthermia. 2006;22(3):191–196.
[4] Horsman MR, Overgaard J. Hyperthermia: a potent enhancer of radiotherapy. Clin Oncol (R Coll Radiol). 2007;19(6):418–426.
[5] Issels RD, Lindner LH, Ghadjar P, et al. 13LBA improved overall survival by adding regional hyperthermia to neo-adjuvant chemotherapy in patients with localized high-risk soft tissue sarcoma (HR-STS): long-term outcomes of the EORTC 62961/ESHO randomized phase III study. Eur J Cancer. 2015;51:S716.
[6] Sherar M, Liu F-F, Pintilie M, et al. Relationship between thermal dose and outcome in thermoradiotherapy treatments for superficial recurrences of breast cancer: data from a phase III trial. Int J Radiat Oncol Biol Phys. 1997;39(2):371–380.
[7] Thrall DE, LaRue SM, Yu D, et al. Thermal dose is related to duration of local control in canine sarcomas treated with thermoradiotherapy. Clin Cancer Res. 2005;11(14):5206–5214.
[8] Franckena M, Fatehi D, de Bruijne M, et al. Hyperthermia dose-effect relationship in 420 patients with cervical cancer treated with combined radiotherapy and hyperthermia. Eur J Cancer. 2009;45(11):1969–1978.
[9] Oei AL, Vriend LEM, Crezee J, et al. Effects of hyperthermia on DNA repair pathways: one treatment to inhibit them all. Radiat Oncol. 2015;10(1):165.
[10] van den Tempel N, Zelensky A, Odijk H, et al. On the mechanism of hyperthermia-induced BRCA2 protein degradation. Cancers. 2019;11(1):97.
[11] Paulides MM, Stauffer PR, Neufeld E, et al. Simulation techniques in hyperthermia treatment planning. Int J Hyperthermia. 2013;29(4):346–357.
[12] Caon M. Voxel-based computational models of real human anatomy: a review. Radiat Environ Biophys. 2004;42(4):229–235.
[13] Iacono MI, Neufeld E, Akinnagbe E, et al. MIDA: a multimodal imaging-based detailed anatomical model of the human head and neck. PLOS One. 2015;10(4):e0124126.
[14] Duan L, Cui S, Xia L. Research on human model construction and electric shock simulation based on difference image and finite element analysis. 2016 ASABE Annual International Meeting. American Society of Agricultural and Biological Engineers; 2016.
[15] Li T, Li Y, Sun Y, et al. Effect of head model on Monte Carlo modeling of spatial sensitivity distribution for functional near-infrared spectroscopy. J Innov Opt Health Sci. 2015;8(5):1550024.
[16] Guérin B, Villena JF, Polimeridis AG, et al. Computation of ultimate SAR amplification factors for radiofrequency hyperthermia in non-uniform body models: impact of frequency and tumour location. Int J Hyperthermia. 2018;34(1):87–100.
[17] Bevacqua MT, Bellizzi GG, Crocco L, et al. A method for quantitative imaging of electrical properties of human tissues from only amplitude electromagnetic data. Inverse Prob. 2019;35(2):025006.
[18] Bevacqua MT, Bellizzi GG, Isernia T, et al. A method for effective permittivity and conductivity mapping of biological scenarios via

segmented contrast source inversion. Prog Electromagnet Res. 2019;164:1–15.
[19] Arayeshnia A, Keshtkar A, Amiri S. Realistic human head voxel model for brain microwave imaging. 2017 Iranian Conference on Electrical Engineering (ICEE). IEEE; 2017.
[20] Paulides MM, Mestrom RMC, Salim G, et al. A printed Yagi-Uda antenna for application in magnetic resonance thermometry guided microwave hyperthermia applicators. Phys Med Biol. 2017;62(5):1831–1847.
[21] Dobšíček Trefná H, Vrba J, Persson M. Evaluation of a patch antenna applicator for time reversal hyperthermia. Int J Hyperthermia. 2010;26(2):185–197.
[22] Vrba D, Rodrigues DB, Vrba J Jr., et al. Metamaterial antenna arrays for improved uniformity of microwave hyperthermia treatments. Prog Electromagnet Res. 2016;156:1–12.
[23] Paulides MM, Numan WCM, Drizdal T, et al. Feasibility of MRI-guided hyperthermia treatment of head and neck cancer. The 8th European Conference on Antennas and Propagation (EuCAP 2014). IEEE; 2014.
[24] Winter L, Özerdem C, Hoffmann W, et al. Design and evaluation of a hybrid radiofrequency applicator for magnetic resonance imaging and RF induced hyperthermia: electromagnetic field simulations up to 14.0 Tesla and proof-of-concept at 7.0 Tesla. PLOS One. 2013;8(4):e61661.
[25] Weihrauch M, Wust P, Weiser M, et al. Adaptation of antenna profiles for control of MR guided hyperthermia (HT) in a hybrid MR-HT system. Med Phys. 2007;34(12):4717–4725.
[26] Bellizzi GG, et al. The potential of constrained SAR focusing for hyperthermia treatment planning: analysis for the head & neck region. Phys Med Biol. 2018;64(1):015013.
[27] Bellizzi GG, Paulides MM, Drizdal T, et al. Sparsity promoted antenna selection in hyperthermia treatment planning. 2018 EMF-Med 1st World Conference on Biomedical Applications of Electromagnetic Fields (EMF-Med). IEEE; 2018.
[28] Bellizzi GG, Crocco L, Battaglia GM, et al. Multi-frequency constrained SAR focusing for patient specific hyperthermia treatment. IEEE J Electromagn RF Microw Med Biol. 2017;1(2):74–80.
[29] Rijnen Z, Bakker JF, Canters RAM, et al. Clinical integration of software tool VEDO for adaptive and quantitative application of phased array hyperthermia in the head and neck. Int J Hyperthermia. 2013;29(3):181–193.
[30] Zhao L, Ye Q, Wu K-L, et al. A new high-resolution electromagnetic human head model: a useful resource for a new specific-absorption-rate assessment model. IEEE Antennas Propag Mag. 2016;58(5):32–42.
[31] Taleb B, Khadour A, Bitar A. Reconstruction of head-to-knee voxel model for Syrian adult male of average height and weight. Egypt J Radiol Nucl Med. 2015;46(2):491–497.
[32] Zastrow E, Davis SK, Lazebnik M, et al. Development of anatomically realistic numerical breast phantoms with accurate dielectric properties for modeling microwave interactions with the human breast. IEEE Trans Biomed Eng. 2008;55(12):2792–2800.
[33] Wang Z, Xiao X, Song H, et al. Development of anatomically realistic numerical breast phantoms based on T1- and T2-weighted MRIs for microwave breast cancer detection. Antennas Wirel Propag Lett. 2014;13:1757–1760.
[34] Zankl M, Wittmann A. The adult male voxel model "Golem" segmented from whole-body CT patient data. Radiat Environ Biophys. 2001;40(2):153–162.
[35] Zubal IG, Harrell CR, Smith EO, et al. Computerized three-dimensional segmented human anatomy. Med Phys. 1994;21(2):299–302.
[36] Gosselin M-C, Neufeld E, Moser H, et al. Development of a new generation of high-resolution anatomical models for medical device evaluation: the Virtual Population 3.0. Phys Med Biol. 2014;59(18):5287–5303.
[37] Christ A, Kainz W, Hahn EG, et al. The Virtual Family-development of surface-based anatomical models of two adults and two children for dosimetric simulations. Phys Med Biol. 2010;55(2):N23–N38.
[38] Fill UA, Zankl M, Petoussi-Henss N, et al. Adult female voxel models of different stature and photon conversion coefficients for radiation protection. Health Phys. 2004;86(3):253–272.
[39] Kok HP, Crezee J. A comparison of the heating characteristics of capacitive and radiative superficial hyperthermia. Int J Hyperthermia. 2017;33(4):378–386.
[40] de Bruijne M, Wielheesen DHM, van der Zee J, et al. Benefits of superficial hyperthermia treatment planning: five case studies. Int J Hyperthermia. 2007;23(5):417–429.
[41] Trujillo-Romero CJ, Paulides MM, Drizdal T, et al. Impact of silicone and metal port-a-cath implants on superficial hyperthermia treatment quality. Int J Hyperthermia. 2015;31(1):15–22.
[42] De Greef M, Kok HP, Bel A, et al. 3D versus 2D steering in patient anatomies: a comparison using hyperthermia treatment planning. Int J Hyperthermia. 2011;27(1):74–85.
[43] Verduijn GM, de Wee EM, Rijnen Z, et al. Deep hyperthermia with the HYPERcollar system combined with irradiation for advanced head and neck carcinoma – a feasibility study. Int J Hyperthermia. 2018;34(7):994–1001.
[44] Ribeiro IVB, van Holthe N, Van Rhoon G, et al. Impact of segmentation detail in hyperthermia treatment planning: comparison between detailed and clinical tissue segmentation. 2018 EMF-Med 1st World Conference on Biomedical Applications of Electromagnetic Fields (EMF-Med). IEEE; 2018.
[45] Ribeiro IVB. Potential impact of MR-only treatment planning for MR guided deep pelvic hyperthermia. 33rd Annual Meeting of The European Society For Hyperthermic Oncology; 2019.
[46] Fortunati V, Verhaart RF, van der Lijn F, et al. Tissue segmentation of head and neck CT images for treatment planning: a multiatlas approach combined with intensity modeling. Med Phys. 2013;40(7):071905.
[47] Verhaart RF, Fortunati V, Verduijn GM, et al. CT-based patient modeling for head and neck hyperthermia treatment planning: manual versus automatic normal-tissue-segmentation. Radiother Oncol. 2014;111(1):158–163.
[48] Verhaart RF, Fortunati V, Verduijn GM, et al. The relevance of MRI for patient modeling in head and neck hyperthermia treatment planning: a comparison of CT and CT-MRI based tissue segmentation on simulated temperature. Med Phys. 2014;41(12):123302.
[49] Burnet NG, Thomas SJ, Burton KE, et al. Defining the tumour and target volumes for radiotherapy. Cancer Imaging. 2004;4(2):153–161.
[50] Canters RAM, Paulides MM, Franckena MF, et al. Implementation of treatment planning in the routine clinical procedure of regional hyperthermia treatment of cervical cancer: an overview and the Rotterdam experience. Int J Hyperthermia. 2012;28(6):570–581.
[51] Goddard M. The EU General Data Protection Regulation (GDPR): European regulation that has a global impact. Int J Market Res. 2017;59(6):703–705.
[52] Turner PF, Tumeh A, Schaefermeyer T. BSD-2000 approach for deep local and regional hyperthermia: physics and technology. Strahlenther Onkol. 1989;165(10):738–741.
[53] Van Rhoon GC, Van Der Heuvel DJ, Ameziane A, et al. Characterization of the SAR-distribution of the Sigma-60 applicator for regional hyperthermia using a Schottky diode sheet. Int J Hyperthermia. 2003;19(6):642–654.
[54] Mulder HT, Curto S, Paulides MM, et al. Systematic quality assurance of the BSD2000-3D MR-compatible hyperthermia applicator performance using MR temperature imaging. Int J Hyperthermia. 2018;35(1):305–313.
[55] Canters RAM, Wust P, Bakker JF, et al. A literature survey on indicators for characterisation and optimisation of SAR distributions in deep hyperthermia, a plea for standardisation. Int J Hyperthermia. 2009;25(7):593–608.

[56] Lee HK, Antell AG, Perez CA, et al. Superficial hyperthermia and irradiation for recurrent breast carcinoma of the chest wall: prognostic factors in 196 tumors. Int J Radiat Oncol Biol Phys. 1998; 40(2):365–375.

[57] Bellizzi GG, Drizdal T, van Rhoon GC, et al. Predictive value of SAR based quality indicators for head and neck hyperthermia treatment quality. Int J Hyperthermia. 2019;36(1):456–465.

[58] van Rhoon GC. Is CEM43 still a relevant thermal dose parameter for hyperthermia treatment monitoring? Int J Hyperthermia. 2016;32(1):50–62.

[59] Kroesen M, Mulder HT, van Holthe JML, et al. Confirmation of thermal dose as a predictor of local control in cervical carcinoma patients treated with state-of-the-art radiation therapy and hyperthermia. Radiother Oncol. 2019;140:150–158.